Wear 530–531 (2023) 204962

Contents lists available at ScienceDirect

Wear

journal homepage: www.elsevier.com/locate/wear

Tool wear and surface integrity in liquid nitrogen clean cutting of cobalt-based superalloy GH605 with AlTiN coated tools

Xiang Li [a,b], Guangming Zheng [a,b,*], Jiwang Yan [c], Xiang Cheng [a], Yang Li [a], Enzhao Cui [a]

[a] School of Mechanical Engineering, Shandong University of Technology, Zibo, 255000, China
[b] Shandong Key Laboratory of Precision Manufacturing and Special Processing, Zibo, 255000, China
[c] Department of Mechanical Engineering, Faculty of Science and Technology, Keio University, 3-14-1 Hiyoshi, Kohoku-ku, Yokohama, 223-8522, Japan

ARTICLE INFO

Keywords:
Liquid nitrogen
Clean cutting
Tool wear
Surface integrity
Cobalt-based superalloy

ABSTRACT

The tool wear is severe and the machined surface quality is low in dry cutting of cobalt-based superalloy. The traditional coolant is harmful to the environment and not in line with sustainable development. The liquid nitrogen (LN_2) clean cutting of cobalt-based superalloy GH605 using AlTiN coated tools is proposed in this work. The tool wear mechanism and the machined surface integrity are investigated. The results show that, with the decrease of LN_2 injection temperature, the sharp wear stage of the tool can be delayed. The injection temperature directly affects the tool life. Compared with dry cutting, the tool life is increased by 42.5% at LN_2 injection of −190 °C. Under the lower liquid nitrogen condition, the coating peeling is reduced on the rake face. The decrease of LN_2 injection temperature can effectively reduce the damaged area of the flank face and inhibit the oxidation wear. The injection temperature between −30 °C and −150 °C can significantly reduce the surface roughness. The minimum surface roughness value at the injection temperature of −90 °C is 0.486 μm, which is 39.4% lower than that at dry cutting condition. When the LN_2 injection temperature is below −90 °C, the thickness of the white layer is less than half of that in dry cutting condition. The hardness of the machined surface is enhanced and the residual stress is reduced at injection temperature below −150 °C. This work demonstrates the possibility of improving the machinability of cobalt-based superalloy by optimizing the LN_2 injection temperature.

1. Introduction

Cobalt-based superalloys usually refer to alloys containing 40%–65% cobalt austenite. In addition, it generally contains 19%–25% Cr element to improve the oxidation resistance and corrosion resistance, 5%–25% Ni element to stabilize the γ austenite matrix can avoid Co element isomerism transformation, 7%–15% W element to play a solid solution strengthening, and a small amount of C element to form carbide [1]. As the melting point of cobalt is 40 °C higher than that of nickel, compared with nickel-based superalloy, the cobalt-based superalloy has higher initial melting temperature, thermal corrosion resistance and fatigue resistance [2–4]. It is widely used in the manufacture of gas turbine blades, engine combustion chambers, turbine disks, and various components in the atomic energy industry under high loads and high temperatures [5,6]. Although the cobalt-based superalloy has an excellent development prospect, its physical and mechanical properties lead to poor machinability. The tool wear is severe and the machined surface quality is difficult to guarantee.

It is well known that metal materials release a lot of heat in the cutting process. Controlling the generation and release of cutting heat can prolong the tool's life and ensure the surface quality of the workpiece. The traditional method of controlling cutting heat is mainly to limit cutting parameters such as cutting speed and feed rate, and to cool/lubricate the cutting region by providing a large amount of cutting fluids. Although these methods, to a certain extent, are effective, they limit production efficiency and increase the production cost. Moreover, the extensive use and discharge of coolant have a negative impact on human health, environment, and resource utilization [7,8]. According to the study of alternative methods to conventional cutting fluid [9], cutting fluids are always contaminated by their use and need to be treated environmentally. The cutting fluid treatment cost accounts for about 17% of the total production cost of the part and nearly six times the total tool cost. With the continuous strengthening of the concept of green manufacturing and sustainable manufacturing, clean-cutting technology has been focused in recent years. This technology includes dry cutting, minimum micro lubrication (MQL), and cryogenic cutting. Under dry

* Corresponding author. School of Mechanical Engineering, Shandong University of Technology, Zibo, 255000, China.
E-mail address: zhengguangming@sdut.edu.cn (G. Zheng).

https://doi.org/10.1016/j.wear.2023.204962
Received 18 January 2023; Received in revised form 13 May 2023; Accepted 16 May 2023
Available online 25 May 2023

cutting, the cutting force is largely due to the lack of cooling and lubrication effects of coolants, and the high cutting temperature dramatically reduces the durability of the tool. MQL technology is to atomize a small amount of lubricating oil into nano-sized particles through an atomizing nozzle. The high-speed injection of oil mist particles into the cutting area provides a good lubrication effect. However, its low cooling capacity cannot effectively remove the cutting heat [10,11]. Therefore, compared with the above two methods, cryogenic cutting is more suitable for machining titanium alloy, superalloy and other difficult-to-machine materials. Thus, the research on cryogenic cutting is increasing.

Cryogenic cutting is a green cutting method that can effectively reduce the cutting temperature by injecting Cryogenic cooling media into the machining area to create a low-temperature or ultra-low-temperature environment in the machining area [12,13]. Common cryogenic cooling media include liquid nitrogen, liquid CO_2, and cryogenic cold air gas. Cryogenic machining can have a favorable impact on cutting temperature, tool wear and machined surface quality [14,15]. Halim et al. [16] studied the high-speed cutting of Inconel 718 using PVD-coated ball-end milling cutters under cryogenic LCO_2 and dry cutting conditions. It was found that severe chip nodules were observed under dry cutting, and the coating peeling continued to expand, accelerating tool wear. Compared with dry cutting, cryogenic LCO_2 significantly increases the tool life by 70.8%. Kumark et al. [17] found that the tool wear of cryogenic LN_2 cutting was 37.5% lower than that of dry cutting when using cemented carbide tools to cut stainless steel. Bermingham et al. [18] studied the tool life and chip morphology of cryogenic LN_2 turning titanium alloy Ti–6Al–4V. Compared with dry cutting, the LN_2 cooling method reduced the chip thickness and tool chip contact length, and the tool life increased by 44%–59%. Wang et al. [19,20] conducted milling experiments on nickel-based superalloy and titanium alloy by cryogenic LN_2 machining method. It was found that the tool produced partial adhesion, diffusion wear and insignificant oxidation wear during cryogenic LN_2 high-speed milling of nickel-based superalloys. Tool life and machining efficiency improved significantly. When cryogenic liquid nitrogen is used to cut titanium alloy, the tool wear is effectively reduced, and the high-frequency vibration at the tooltip is reduced. Moreover, the cooling effect of LN_2 external spraying on the surface quality of high-speed cutting is better than that of LN_2 internal spraying. Danish et al. [21] and Jerold et al. [22] carried out cutting experiments on Inconel 718 and titanium alloy under cryogenic LN_2 and cryogenic LCO_2, respectively. The results show that the cutting effect of cryogenic LN_2 is better than that of cryogenic LCO_2. The liquid nitrogen cooling environment can significantly reduce the cutting force, tool wear and surface roughness.

Compared with LCO_2, LN_2 as a cooling medium can substantially reduce the cutting temperature, which is a commonly used clean cooling medium [23]. Nitrogen is abundant and chemically stable, and it evaporates quickly into the air during use without causing pollution to the environment [24]. When liquid nitrogen is used as a cooling and lubricating medium, the very low temperature reduces the plasticity of the material and contributes to the machinability of the workpiece [25]. Moreover, the environmental, economic and technological sustainability of cryogenic processing techniques is studied [21]. They pointed out that the cryogenic LN_2 cutting method is more sustainable than other cooling methods. However, there is no life cycle analysis in the use of cryogenic LN_2 coolant cutting. Life cycle analysis plays an important role in reducing energy consumption, shortening the product development cycle, improving product market competitiveness, and protecting human health and the ecological environment [26]. The performance and life cycle analysis of end milling under dry and LCO_2 cutting conditions is also investigated [27]. It is found that the lower power consumption, better surface roughness and high tool life can be obtained, when the LCO_2 is used as a cutting fluid instead of dry machining. It is also a real improvement from an environmental point of view. In terms of environmental impact and human health, compared with other coolants, the cryogenic LN_2 cutting method has become a suitable alternative for the industrial processing of difficult-to-machine materials.

At present, the tool materials commonly used in high-speed cutting superalloys include cemented carbide tools, coated cemented carbide tools, cermet tools, ceramic tools and PCBN tools [28,29]. However, there are limited kinds of reference tools for the cryogenic cutting of superalloys. Coated tools are often used in cryogenic cutting environments because of their excellent economy, high wear resistance, high chemical stability, low friction coefficient and long service life. Studies have shown that when cutting superalloys with LN_2 and LCO_2 at cryogenic, the primary wear forms of coated tools are coating spalling, groove wear, bond wear, and blade collapse [30–32].

According to the literature review, the research on machining superalloys in a cryogenic cutting environment mainly focuses on nickel-based superalloys, while that on cobalt-based superalloys is very little. Moreover, although there have been investigations on the cooling performances of different cooling media, research on the cutting mechanism of superalloy machining at different temperatures of a certain cooling medium is still rare. In this work, cobalt-based superalloy GH605 is taken as the workpiece material. High-speed milling experiments are performed using PVD-AlTiN coated tools under LN_2 cooling at different injection temperatures. The influence of different injection temperatures on tool wear and machined surface integrity including surface roughness, white layer microstructure, microhardness, and surface residual stress of coated tools are examined. The result is also compared with that obtained by dry cutting, in order to investigate the special features of cryogenic cutting with LN_2. This work provides important theoretical support and technical evidence for the clean cutting of difficult-to-machine materials.

2. Material and methods

2.1. Workpiece and tool materials

The cobalt-based superalloy GH605 with a hardness of 32±1HRC was used as the workpiece material, and its initial size was 105 mm × 100 mm × 80 mm. The main chemical compositions were shown in Table 1, which was measured by CATC Technology Innovation (Beijing) Corporation Materials Testing Laboratory. Fig. 1 presents the microstructure and tensile stress-strain curve of GH605. The microstructure was observed by Quanta 250 scanning electron microscopy (SEM) with an energy dispersive spectrometer (EDS). The tensile strength and yield strength of GH605 were tested by MTS810 electronic universal testing machine. To ensure the reliability of the test results, three tensile samples were selected to draw the tensile stress-strain curve, as shown in Fig. 1b. From the tensile test results, the average yield strength of cobalt-based superalloy is about 460 MPa and the tensile strength is 970 MPa.

The PVD-AlTiN coated cemented carbide inserts (KC522 M), which are produced by Kennametal Company (USA), are selected as cutting tools. The product type of the insert is EDCT10T304PDERLD. For this insert, two cutting edges are involved at the same time in the cutting process. The geometric parameters of the insert KC522 M are shown in Table 2. The tool holder model is 20A03R028A20ED10, and the diameter of the tool holder is 20 mm.

2.2. Liquid nitrogen clean cutting experiment

Fig. 2 shows the experimental setup and system structure. As can be seen from Fig. 2a and b, the milling experiment was carried out on a 5H machine produced by Beijing Yiji Precision Machine Tool Co., Ltd. Combined with the recommended value of the tool manual and literature reference about the cutting of such cobalt-based superalloy material, the cutting parameters (cutting speed $v_c = 117$ m/min, the axial cutting depth $a_p = 0.2$ mm, the radial cutting depth $a_e = 3$ mm, and the feed per tooth $f_z = 0.09$ mm/z) are selected after several trial cutting

Table 1
Main chemical composition of GH605 (wt%).

C	Cr	Ni	W	Co	Mn	Fe	Si	P	S
0.096	19.66	10.46	14.95	Bal	1.55	2.11	≤0.2	≤0.04	≤0.03

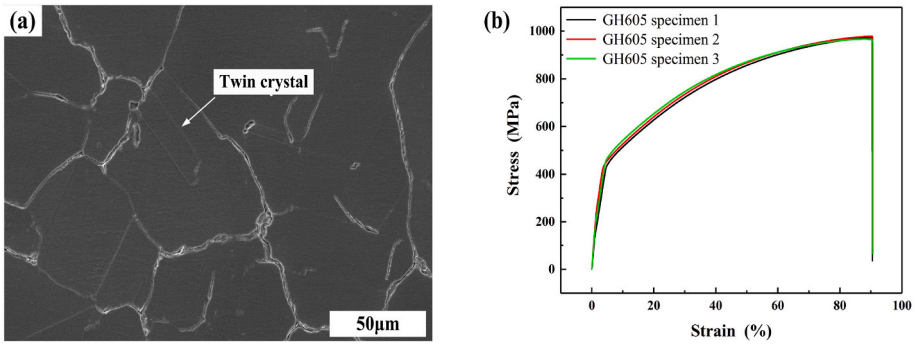

Fig. 1. (a) Microstructure and (b) Tensile stress-strain curve of GH605.

Table 2
Geometric parameters of the insert KC522 M.

Rake angle γ_o (°)	Clearance angle α_o (°)	Inclination angle λ_s (°)	Corner radius r_ε (mm)	Length L (mm)	Thickness S (mm)
8°	15°	15°	0.4	12.05	3.75

tests. In the liquid nitrogen cryogenic jet milling experiment, the liquid nitrogen injection temperature is set to −30 °C, −90 °C, −150 °C and −190 °C. Dry cutting conditions are selected for comparison (counted as 20 °C). The liquid nitrogen cryogenic cooling system adopts a circular liquid nitrogen nozzle with a diameter of 4 mm.

The influence of the variation of the cryogenic cooling cutting system on the tool life during the cutting process was considered. To ensure the rigor and reliability of the test, the fixed nozzle position and the same injection area and injection target distance are used. The liquid nitrogen is directly transported to the cutting area through the nozzle during the

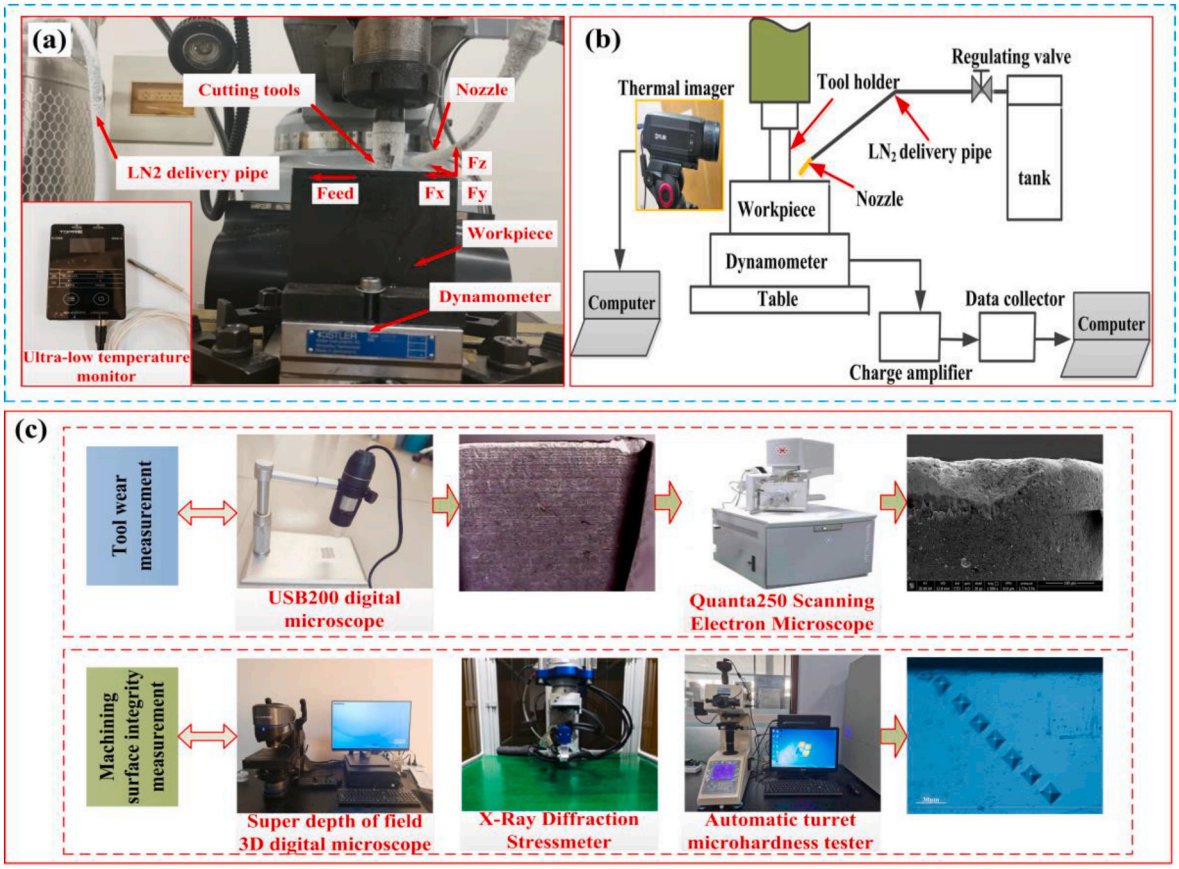

Fig. 2. Experimental system construction. (a) Experimental setup, (b) Measurement system, and (c) Main measurement instruments.

cutting process. The nozzle position is 25 mm from the chip contact area. To ensure the constant pressure of the self-pressurized liquid nitrogen tank in the test, the pressure threshold was maintained at about 0.2 MPa, and the injection flow was controlled at 0.4–0.8 L/min. BD-200A liquid nitrogen tank ultra-low temperature monitor was used to measure the liquid nitrogen temperature at the nozzle.

2.3. Measurement equipment and method

In the cutting test, in order to avoid too many inserts affecting the accuracy of the test results, the tool holder is only clamped with one insert. After each milling length of 100 mm, the flank wear was measured by USB200 digital tool microscope. The cutting temperature was measured by FLIR A615 infrared thermal imager manufactured by FLIR SYSTEMS. The change in cutting temperature was recorded in real-time by Flir Tools + software. The thermal imaging camera needs to be calibrated and calibrated prior to the dry/cryogenic cutting experiment. In order to measure the temperature accurately, the influence of various different radiation sources must be considered. This compensation operation is done automatically by the thermal imaging camera online. It is also necessary to complete the cutting temperature measurement by providing parameters such as the emissivity of the object (0.95), the distance between the object and the camera (1 m), and the atmospheric temperature to the thermal imaging camera (20 °C).

The Kistler 9257B piezoelectric dynamometer was used to measure the cutting force. Each cutting fraction force was selected for the same wear of the tool at $VB = 0.3 \pm 0.01$ mm. The force signal data were collected by DEWESoft software. The jet pressure generated by the nitrogen flow ejected at the nozzle has some influence on the cutting force during the cutting process. Compared with the cutting forces caused by the deformation and friction, however, the cutting force caused by the nozzle spray is smaller. The pressure generated at the nozzle is not significant and it is not a major influence. Therefore, the influence of cutting force caused by the nozzle spray was not considered in this work.

The workpiece sample was cut into 10 mm × 8 mm × 8 mm at the cross-section, to analyze the machined surface integrity of GH605. According to the indentation method, the microhardness of GH605 machined surface was tested by HVS-1000A automatic turret microhardness tester. The microhardness of GH605 machined surface is larger. Due to reducing the measurement error value and obtaining a larger indentation diagonal, the load of 9.8 N (1 kgf) and the holding time of 15 s was used for measuring the microhardness of the machined surface. For the microhardness measurement in the depth direction, the measurement starts at about 5 μm from the machined surface on the cross section, which was performed every 15 μm along the depth direction. At this time, in order to obtain the depth of the hardened layer more accurately, and ensure the indentation depth and diagonal length within the maximum allowable error range of the measuring instrument, the load of 0.98 N (0.1 kgf) and the holding time of 15 s was used. Multiple measurements were performed at different positions on the same surface. And then the average value was taken as the surface microhardness value under this parameter. The X-ray diffraction stress meter of Stresstech X-stress 3000 G2R is used to test the residual stress on the surface of the sample. The X-ray residual stress test parameters are exhibited in Table 3. The equipment is calibrated and measured. Three measuring points are evenly selected along the feed direction and the vertical feed direction of the machined surface of the piece. The average value of the measured results is taken. Surface roughness was measured by a DSX1000 super depth of field 3D digital microscope. Meanwhile, the Quanta250 scanning electron microscope (SEM) was used to observe the wear morphology of the tool surface and the microstructure of the processed white layer. The element distribution on the surface was analyzed by EDS. The Experimental measuring instruments are presented in Fig. 2c.

Table 3
X-ray residual stress test parameters.

Parameters	Value
Testing method	tilt fixing Ψ
X-ray wavelength (nm)	0.2291
Target materials	Mn
Operating voltage (kV)	30
Diffraction Angle (°)	152.3
diameter of collimator Φ (mm)	2
Angle of bank(°)	0,26.4,39
Diffraction crystal plane	311
Operating current (mA)	6.6
Exposure time (s)	30

3. Results and discussion

3.1. Cutting force and cutting temperature

The effect of liquid nitrogen injection temperature on cutting force is shown in Fig. 3. F_z (axial force) is the largest component of the cutting force, that is, the main cutting force. This is consistent with the research of Li et al. [33], which indicates that the extrusion and friction between the flank face of the coated tool and the workpiece are more significant than that between the rake face and the workpiece. The influence of injection temperature on the cutting force in three directions is basically the same.

The cutting force decreases first and then increases with the decrease of temperature (Fig. 3). Under the dry milling condition, due to the absence of cooling and lubrication of the cooling medium, the temperature of the cutting area increases. The tool edge passivation is serious. And the contact area of the tool-chip interface increases, which makes the contact part have a strong friction effect. Thus, the cutting force is larger. Under the liquid nitrogen condition, the minimum and maximum main cutting force is obtained at −30 °C and −190 °C, respectively. At −30 °C, the injection temperature is not very low, and the nitrogen flow has a good lubrication effect. Compared with dry cutting, the deformation of the serrated chip is smaller at −30 °C, and the chip is easier to break. The force produced by plastic deformation at the chip separation is reduced [34]. With the decrease of injection temperature, the cutting force increases gradually. The reason is that the lower the injection temperature is, the lower the cutting temperature is. The machined surface is gradually in a low-temperature state. Due to the increase in cold deformation, the surface hardness and strength of cobalt-based superalloy are improved. Therefore, a large milling force is needed to

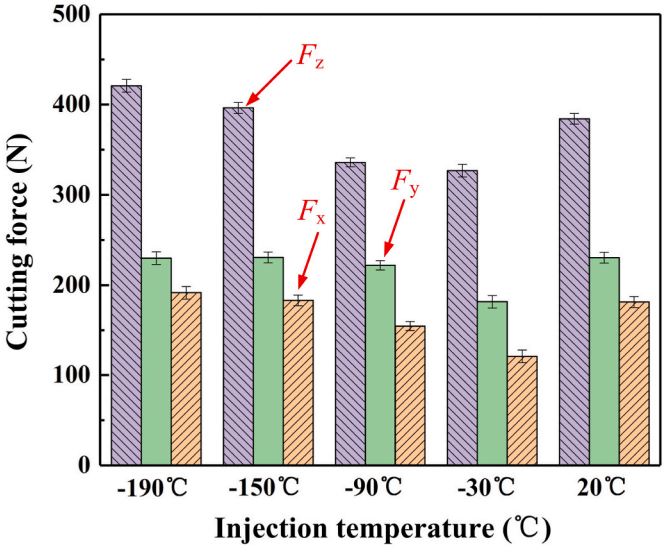

Fig. 3. Effect of injection temperature on cutting force.

remove the material in the cutting process. On the other hand, a lower injection temperature requires a larger liquid nitrogen flow rate, which makes the liquid nitrogen flow rate of the pipeline conveying liquid nitrogen increases sharply under the unit cross-sectional area. The liquid nitrogen sprayed at the nozzle will also have a certain impact on the cutting force under the action of high flow rate and pressure, resulting in an increasing by cutting force.

By measuring the temperature in the cutting area, it can be observed that the higher temperature area is mainly concentrated in the contact position between the tool tip and the workpiece. Fig. 4 exhibits the effect of injection temperature on cutting temperature. With the decrease of injection temperature, the cutting temperature is reduced gradually. The highest cutting temperature is obtained under the dry cutting condition, because there is no lubrication and cooling during the cutting process, resulting in a large amount of cutting heat accumulation on the tool-workpiece contact surface. According to the real-time monitoring of the infrared thermal imager in the cutting process, the cutting temperature at dry cutting conditions has been in a relatively stable concentration and repeated staggered state. So, the cutting temperature is high in dry cutting conditions. At injection temperature of −30 °C, the maximum temperature drops to 130 °C in the cutting zone, which declines by nearly 50%, compared with that at dry cutting conditions, some of the heat generated by tool cutting is absorbed by the nitrogen gas flow. And the gas permeability is strong, reducing the cutting temperature. At the injection temperature of −90 °C, the cutting temperature at the tool's tip decreases significantly. The highest cutting temperature occurs when the tool has just entered the cutting process stage, because of intermittent milling. The tool-workpiece contact is impacted and produces a relatively high temperature. In the subsequent milling process, the larger injection pressure makes the chips leave the cutting area more quickly and the heat cannot accumulate. In addition, the emitted cutting heat is largely balanced by the ejected nitrogen flow. As the liquid nitrogen injection temperature decreases, the cutting area at −150 °C and −190 °C is already in a local low-temperature state. In this state, the low-temperature brittleness of the material makes the surface of the chip more prone to cracks. The separation of chips and workpieces is accelerated, and the tool wear is reduced effectively.

3.2. Tool life and wear mechanisms

The effect of injection temperature and cutting length on flank wear of AlTiN coated tool is displayed in Fig. 5. With the increase of milling length, the wear rate of the coated tool is the fastest in dry milling. When the milling length is 1575 mm, the wear of the tool flank first reaches the failure standard $VB = 0.3$ mm. With the decrease of liquid nitrogen injection temperature, the slope of the flank wear curve decreases gradually. In the initial wear stage, the tool wear increases rapidly and the milling distance is short, which belongs to the rapid growth wear state. In the same milling length ($L = 300$ mm), the flank wear at dry cutting and cryogenic liquid nitrogen cutting is relatively uniform. The tool wear is large under dry cutting. There is slight chipping at the tip of the flank. The rake face also appears to have a passivation phenomenon. However, the tool wear is significantly smaller at liquid nitrogen injection of −150 °C. It is indicated that the use of a cooling medium has affected the tool wear from the initial stage.

In the steady wear stage, the cutting tool maintains a stable wear rate. In the sharp wear stage, the wear curve increases sharply and the slope of the curve is the largest in dry cutting conditions. Under liquid nitrogen cryogenic cutting conditions, the process of the tool entering the rapid wear stage is greatly delayed with the decrease of injection temperature. When the tool reaches the failure standard, the milling length is larger. And the tool life is improved. When milling length $L =$ 1700 mm, the dry cutting tool has exceeded the wear failure standard. The flank cutting edge wear is uneven, and severe damage occurs near the tooltip. However, under the condition of liquid nitrogen injection cutting at −150 °C, uneven wear also occurs. However, the flank face is basically intact. The phenomenon of adhesive accumulation can be seen from the rake face. Due to the periodic change of thermal load and mechanical load during the milling process, high pressure and friction may be generated when the cutting edge of the tool comes out. The unstable build-up layer may not be blown away by the liquid nitrogen stream. Eventually, the tool's substrate surface is not exposed.

The wear morphology of the tool rake face at injection temperatures of 20 °C, −90 °C and −190 °C is presented in Fig. 6 (cutting length $L =$ 1700 mm). The rake face has been damaged to varying degrees. By comparison, the tip breakage of the rake face is the most obvious in dry milling conditions (Fig. 6a), with a larger damage area and deeper groove. Moreover, the cutting edge of the tool is accompanied by the formation of the built-up edge under dry milling conditions. The damage at the tooltip and the existence of the built-up edge change the actual position of the tooltip. The mechanical stress and thermal stress concentration occur on the rake face or rake face away from the cutting edge. At the same time, a certain vibration will be generated in the processing, which will affect the surface quality and dimensional accuracy of the workpiece. When the injection temperatures are −90 °C and −190 °C, the damage degree of the tooltip is significantly reduced. Especially, the damage degree of the rake face is the smallest at −190 °C. The chip bonding phenomenon appeared at the edge of the tool breakage at −90 °C, and the coating is obviously peeled off. With the decrease of the injection temperature, the temperature of the cutting area is gradually decreased. The adhesion of the workpiece material attached to the rake surface will be removed by the liquid nitrogen airflow with a higher flow rate. Therefore, it is not easy to produce chip nodules and chip bonding on the rake face in a low injection environment. At the same time, a gas-liquid mixed protective film can be formed on the tool's surface, which can enhance the lubrication effect near the cutting edge. The friction coefficient between the tool and the workpiece is decreased, thereby reducing tool wear.

EDS of region A in Fig. 6b and region B in Fig. 6c is exhibited in Fig. 7. The elements of Co, Cr, Ni, and Cr appear near the damage of the

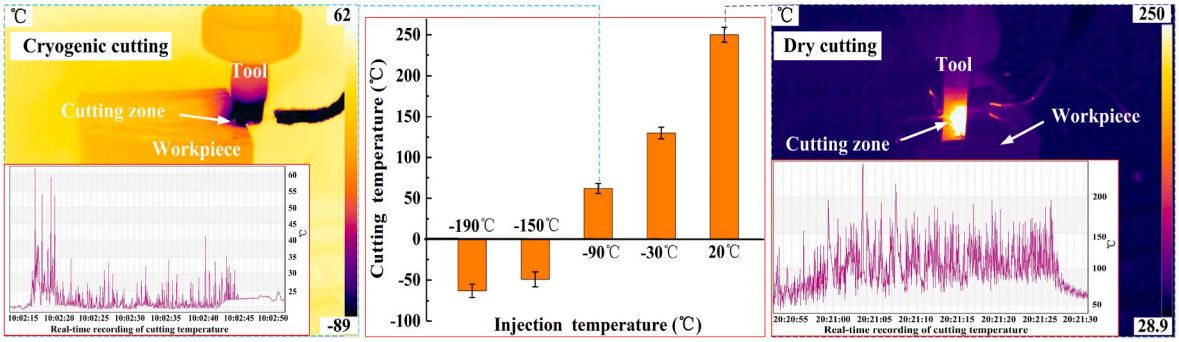

Fig. 4. Effect of injection temperature on cutting temperature.

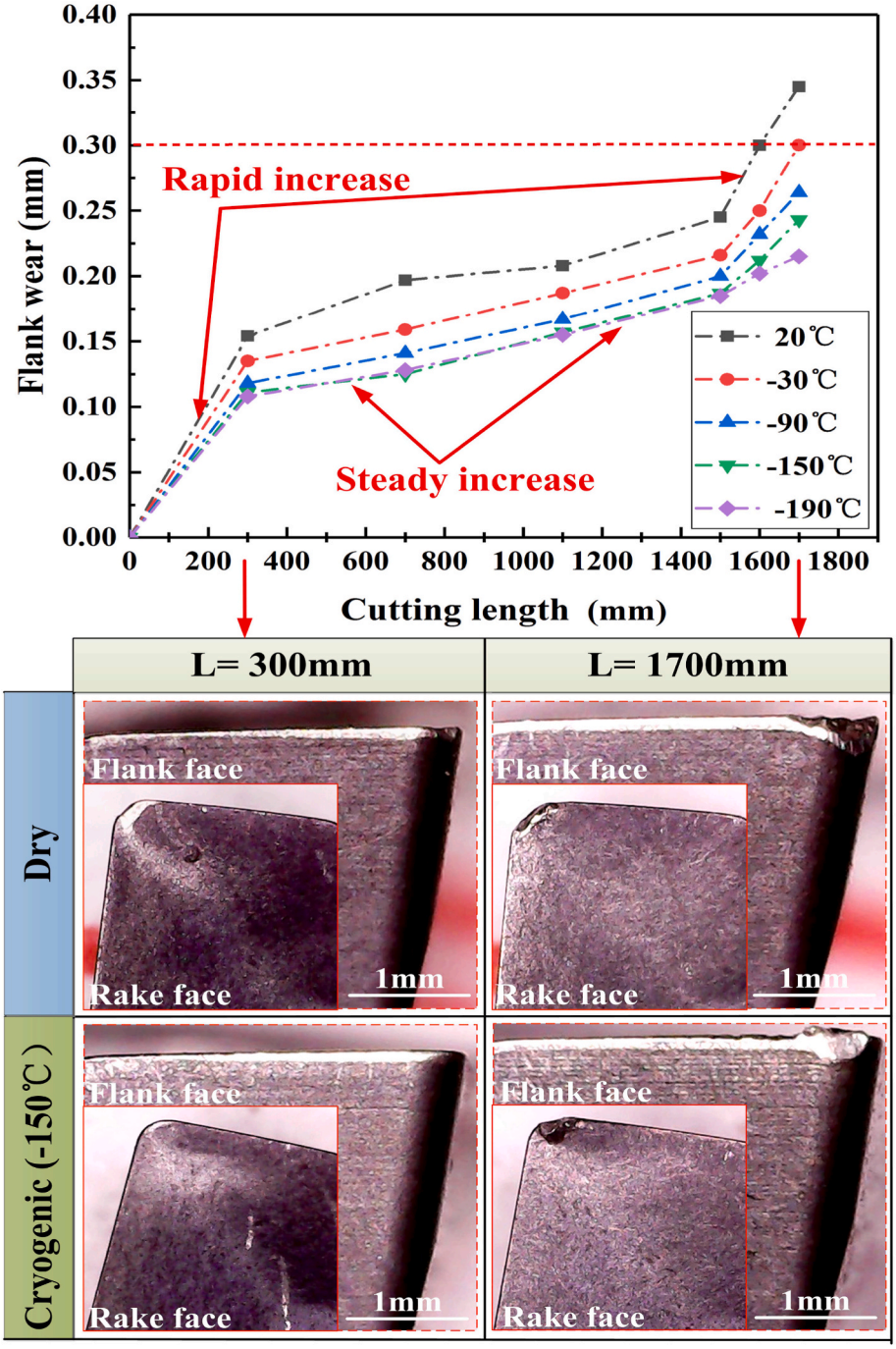

Fig. 5. Effect of injection temperature and cutting length on flank wear of AlTiN coated tool.

tool rake face under liquid nitrogen injection, which proves that adhesive wear occurs. In dry cutting conditions, the high friction and high load are generated by the chip adhesion on the tool-chip interface. When the high temperature and high pressure of the interface reach the critical level, the material bonded on the tool surface will be taken away by the chip flow. Moreover, part of the tool material may be taken away, resulting in a large area of shedding. Thus, the tool adhesive wear is aggravated. In liquid nitrogen cutting conditions, effective cooling and lubrication keep the interface temperature at a low state when the binder is not blown away by the nitrogen flow. The workpiece material will firmly adhere to the rake face, which can play a certain protective role. However, this protection is more effective when the liquid nitrogen injection temperature is low. W element content at region A at −90 °C is much higher than at −190 °C (Fig. 7). The coating peeling is more severe at −90 °C, resulting in substrate exposure. Therefore, the tool substrate can be protected at a lower liquid nitrogen injection temperature. Moreover, the peeling of the coating is reduced. The degree of tool breakage is delayed.

The wear morphology of the tool flank face at injection temperatures of 20 °C, −30 °C, −90 °C, −150 °C and −190 °C is shown in Fig. 8 (cutting length $L = 1700$ mm). There is a certain degree of tool breakage on the flank face. As can be shown in Fig. 8a, the large area of tool breakage and the broad furrow fringes are generated under dry cutting conditions, accompanied by chip bonding, cracks and chipping. Large cracks are observed along the vertical direction of the cutting edge. The main reason is that the coating has been completely peeled off. At the

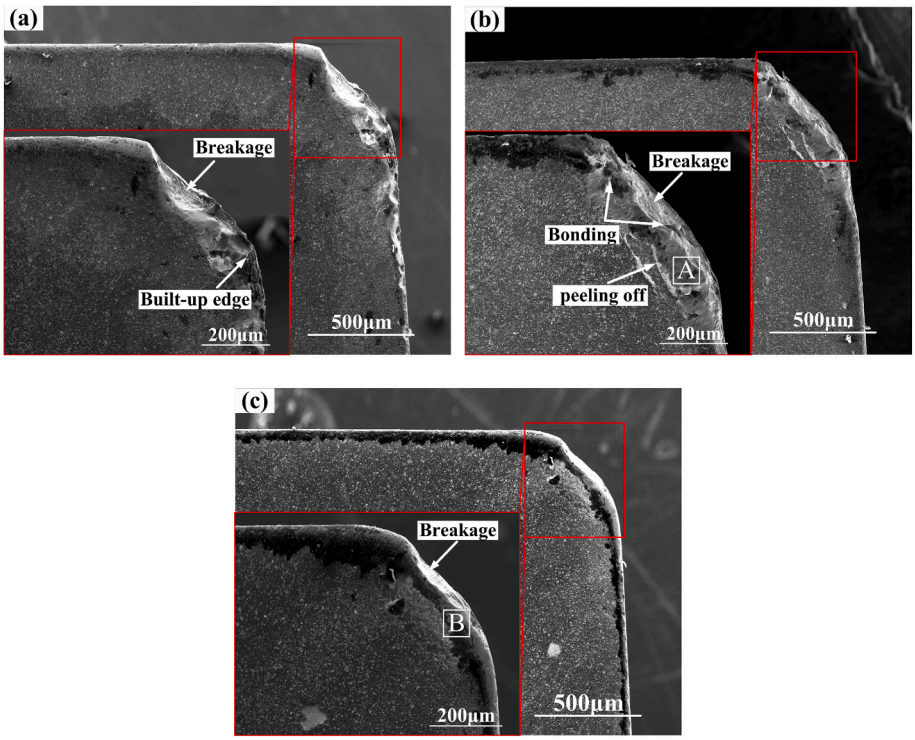

Fig. 6. Wear morphology of tool rake face at injection temperatures of (a) 20 °C, (b) −90 °C and (c) −190 °C (v_c = 117 m/min, f_z = 0.09 mm, a_p = 0.2 mm, a_e = 3 mm).

same time, the substrate lacks the protection of the external coating. The large wear and cracks are found at the edge, due to the high-frequency mechanical impact. In addition, the adhesion near the crack in the damaged area adheres to the tool's surface. This intensifies the adhesive wear. EDS analysis of the C region in Fig. 8a is shown in Fig. 9a. There is a high content of the O element, indicating that oxidation wear occurs on the flank face under the high cutting temperature.

Compared with dry cutting, with the decrease of injection temperature, the damaged area is reduced significantly. At the injection temperature of −30 °C and −90 °C, the damaged area of the cutting edge along the flank is significantly reduced, and the undamaged area is accompanied by coating peeling and scratch (Fig. 8b and c). The scratch is induced by the hard particles in the workpiece. At −150 °C, the build-up layer appears on the cutting edge (Fig. 8d). As shown in Fig. 9b, the high content of Co, Cr and other elements in the layered area is found. It indicated that the workpiece material adheres to the tool face as a build-up layer. There is a certain protective effect in the cutting process. However, as the cutting progresses, when the bonding force between the layer and the tool-worn surface is less than the shear force generated by the outward flow of the chip. The bulk material stacked on the flank face will be carried away by the chip flow along the crack. Then, the cutting performance of the tool is reduced and the tool wear is increased. The damaged area at −190 °C is smaller than that at other injection temperatures. Therefore, the tool wear rate is alleviated effectively with the decrease of liquid nitrogen injection temperature.

The wear morphology and EDS of tool flank wear (VB = 0.180 mm) at injection temperature of −150 °C is presented in Fig. 10. There is no tool breakage on the flank. Area E is mainly composed of Co, Cr and other elements of workpiece elements, indicating that the workpiece materials are bonded near the cutting edge of the tool. The noticeable bonding wear occurs near the cutting edge. The tool's main matrix element of W is presented in area F, due to the coating peeling. Compared with area G, it is obvious that the main elements in the intact coating area are Al, Ti and N coating elements.

3.3. Surface roughness and topography

The effect of injection temperature on the machined surface roughness S_a and 3D surface topography (tool flank wear VB = 0.2 mm) is exhibited in Fig. 11. The surface roughness decreases first and then increases with the decrease of injection temperature. The three-dimensional morphology is relatively flat, mostly showing a yellow-green state. In dry milling conditions, the maximum surface roughness is 0.802 μm, and the color of surface morphology is blue, purple and red. It is indicated that the flatness decreases, and the surface undulation increases.

Compared with dry cutting, the minimum surface roughness of 0.486 μm is obtained at −90 °C, which is reduced by 39.4% (Fig. 11). When the liquid nitrogen injection temperature is −30 °C, −150 °C and −190 °C, the surface roughness is reduced by 30.55%, 28.18% and 22.07%, respectively. This is mainly due to the good cooling and lubrication effect of liquid nitrogen. The high-frequency vibration is reduced at the tooltip, thereby diminishing the machining surface roughness. When the temperature is too low, however, the surface roughness value increases. The reason may be that the decrease of the injection temperature makes the surface hardness increase, and the hard particles in the material have severe friction with the tool flank. Therefore, high surface quality is achieved at injection temperatures between −30 °C and −150 °C.

3.4. Surface/subsurface damage

The effect of injection temperature on the white layer microstructure and element weight ratio of GH605 is displayed in Fig. 12. The machined surface layer of GH605 has obvious delamination along the depth direction. The white layer is uniformly distributed and highly dense in the upper layer. Moreover, the plastic deformation zone with obvious deformation in the metamorphic layer is below the white layer, which is the transition zone. As the depth from the machined surface increases, the substrate material is below the dark layer. The existence of a white

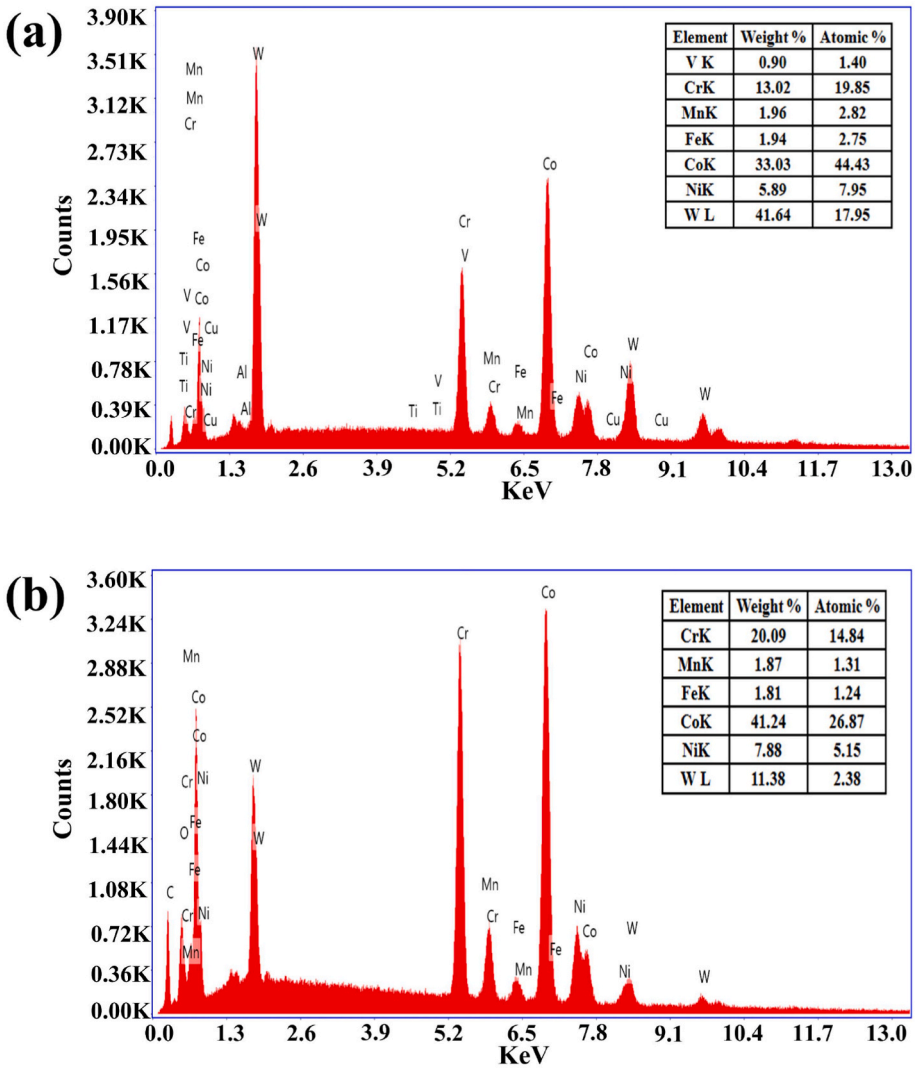

Fig. 7. EDS of (a) region A in Fig. 6b and (b) region B in Fig. 6c.

layer on the machined surface has an important influence on the surface quality. The white layer has great brittleness, which can make the machined surface easy to form cracks and affects the fatigue life of the workpiece. Additionally, the high hardness of the white layer can improve the corrosion resistance and wear resistance to a certain extent.

The thickness of the white layer is 4.506 μm, 1.863 μm and 1.619 μm at dry milling conditions, liquid nitrogen injection temperature −90 °C and −190 °C, respectively. When high-speed dry milling of GH605, the thickness of the white layer is much larger than that of under liquid nitrogen injection cutting conditions. A large amount of cutting heat is generated in the dry cutting process and gathered in the machining surface. Under the coupling effect of high strain and high temperature, the deformation resistance of the workpiece is reduced. The plastic hardening caused by mechanical load and the softening effect caused by thermal load jointly act on the machined surface. Subsequently, these effects increase the penetration depth along the cutting depth direction. Thus, a thicker white layer is formed (Fig. 12a).

On the other hand, under the liquid nitrogen cryogenic injection cutting condition, the white layer is induced mainly by the plastic deformation caused by high mechanical load contact. The slip line can be clearly seen in the transition zone (Fig. 12b and c), which indicates the plastic deformation. However, the microstructure of the transition zone is relatively coarse, and the grain boundary area is obviously increased under dry cutting conditions. This is due to the severe plastic deformation of the machined surface, resulting in lattice distortion and distortion. Moreover, the shear slip grains between grains are elongated and fibrosis.

When it comes to the application of cobalt-based superalloys, the presence of white layers will lead to fatigue failure of key aerospace structural components. Therefore, it is very important to reduce the thickness of the white layer. In this work, a smaller white layer thickness is obtained when the liquid nitrogen injection temperature is −190 °C. During cryogenic cutting of Inconel 718, the reduction of white layer grain structure deformation is presented [35], which is also consistent with this work. At the same time, the use of appropriate post-processing techniques, such as shot peening, can improve the functional performance of advanced materials after material removal [36], and further remove or minimize the effect of the white layer on the fatigue life of the workpiece.

The contents of C and O elements in the white layer of GH605 are detected (Fig. 12d). The content of C elements in the white layer of GH605 after liquid nitrogen injection milling at −190 °C is reduced, and even the existence of O element is not detected. This shows that the contents of oxides and carbides in the white layer of the dry milling surface are more. During the dry milling process, the elements in the alloy react with the C, O and other elements in the air at high temperature and high pressure. In the liquid nitrogen cutting process, however, liquid nitrogen gasification can not only absorb a large amount of heat

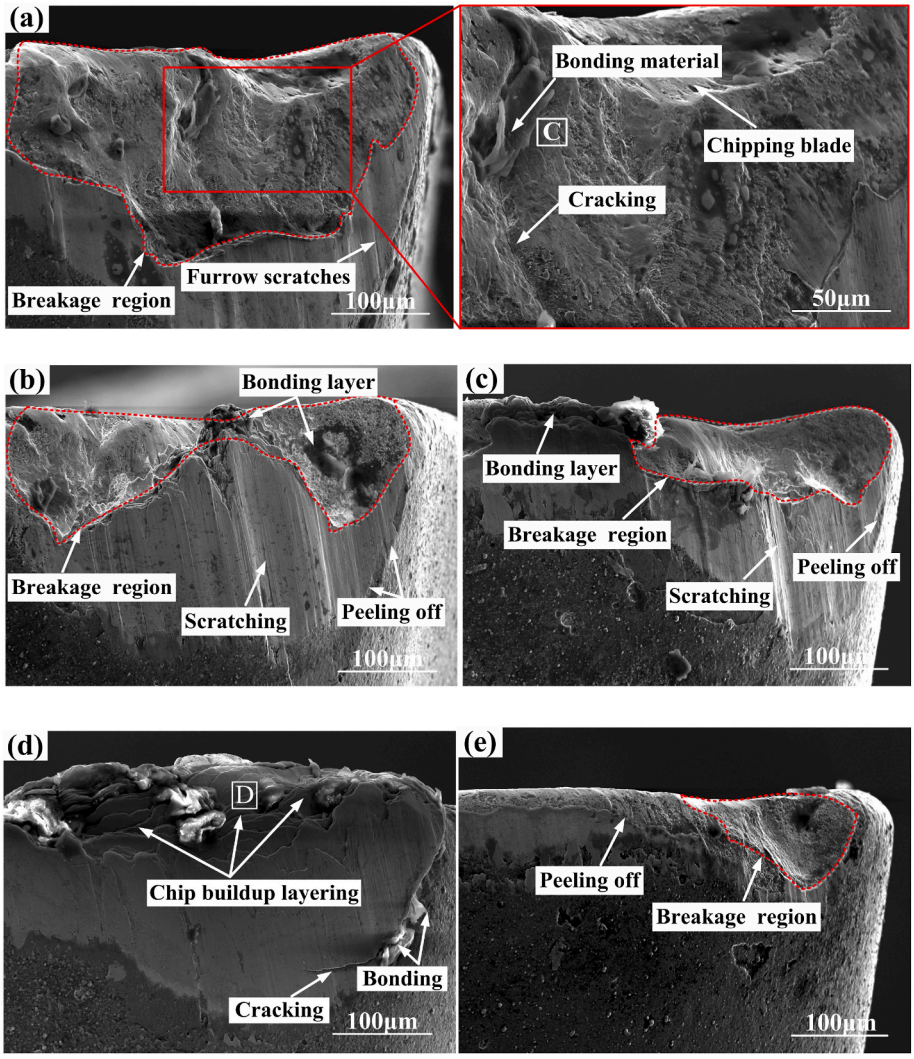

Fig. 8. Wear morphology of tool flank face at injection temperatures of (a) 20 °C, (b) −30 °C, (c) −90 °C, (d) −150 °C and (e) −190 °C.

but also effectively suppress the temperature rise in the cutting area. Moreover, the formed liquid-gas buffer layer can play a role in lubrication, reducing the friction coefficient contact between the tool and the workpiece. Thus, the generation of plastic deformation on the machined surface is reduced.

3.5. Surface hardness and residual stress

The effect of injection temperature on the machined surface hardness of GH605 is shown in Fig. 13. The cobalt-based superalloy GH605 has a serious work hardening phenomenon. Deformation of GH605 causes lattice distortion in the cutting process. And the grains are elongated or even broken, which will hinder the further deformation of GH605 from strengthening and improving the hardness of the material. With the decrease of injection temperature, the machined surface hardness of GH605 generally shows a gradual upward trend. The microhardness of the machined surface at −190 °C is 411.9 HV and 455 HV when the cutting length is 50 mm and 1450 mm, which is enhanced by 9.6% and 15.5%, respectively, compared with dry milling condition (20 °C).

Under the dry cutting conditions, the cutting heat will act on the machined surface, which will soften the surface layer of the material and reduce the degree of work hardening. Under liquid nitrogen cooling conditions, the machined surface is in a low-temperature state. The effect of cutting heat will be offset. However, the low temperature enhances the strength of the material, and the cutting force increases. The surface hardness of the alloy material is further improved due to the increase of cold deformation. The hardness of the machined surface has little change at −90–20 °C. Reasonable cooling is also beneficial to reduce the plastic deformation caused by the thermal effects. So, it has little impact on the change of microhardness.

The change of microhardness along the direction of work hardening depth is shown in Fig. 14. Under dry cutting and liquid nitrogen cryogenic injection cutting conditions, the hardness value of the machined surface is much greater than that of the subsurface region. With the increasing depth from the machined surface, the hardness of the surface layer gradually decreases to the hardness value of the base material at the depth of about 50 μm. Secondly, the dry cutting condition is subject to the thermal effect, and the hardness value of the subsurface area near the machining surface is lower. Under the liquid nitrogen cryogenic injection cutting conditions, the subsurface area near the machined surface is more severe work hardening due to the influence of low-temperature machining.

The effect of injection temperature on the surface residual stress of GH605 is presented in Fig. 15. With the decrease of injection temperature, the residual stress on the machined surface of cobalt-based superalloy GH605 first increases and then decreases. The formation of residual stress on the machined surfaces is mainly affected by mechanical stress and thermal stress [37]. In dry milling of GH605, the tool-workpiece interaction is strongly affected by friction, and the surface temperature increases. The temperature of the inner layer of the

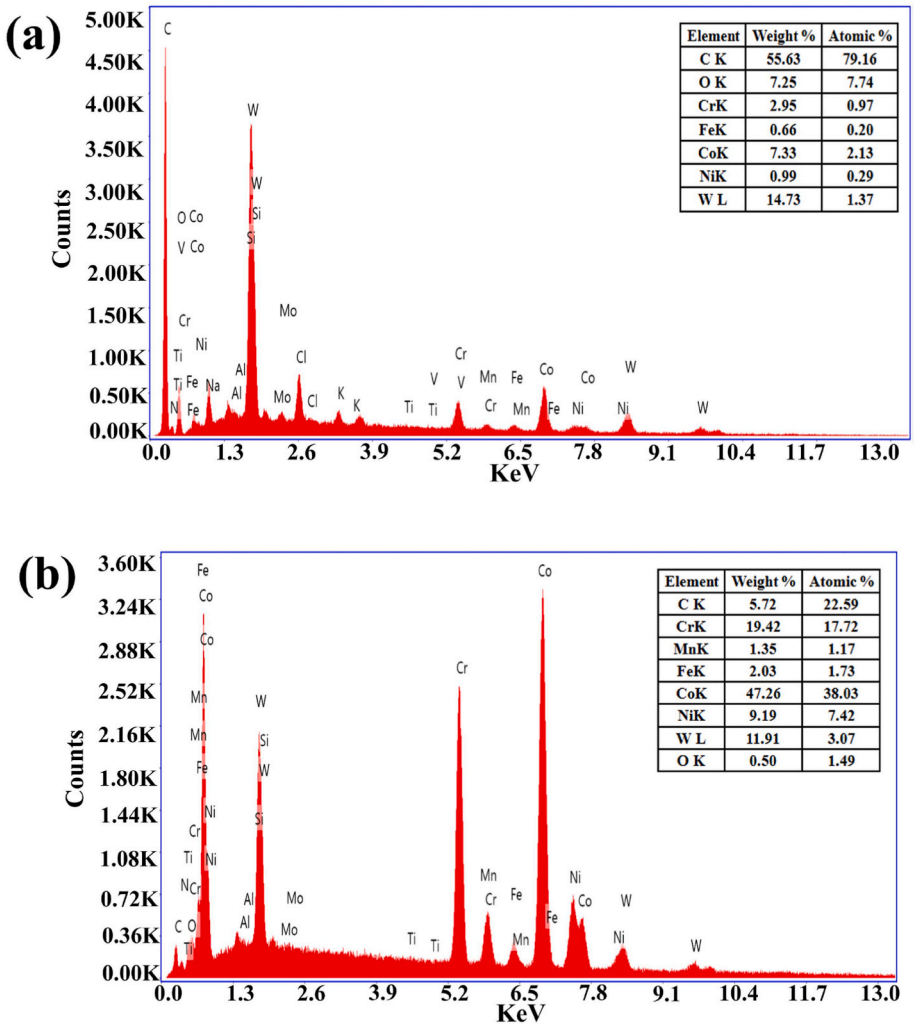

Fig. 9. EDS of (a) region C in Fig. 8a and (b) region D in Fig. 8d.

workpiece is relatively low, which is subjected to an uneven thermal effect, resulting in thermal stress. The machined surface layer is plastically deformed. After recovering room temperature after cutting processing, the surface layer and the inner layer decrease to the same temperature. The shrinkage of the surface layer is large and that of the inner layer is small. The shrinkage of the surface layer is restricted by the inner layer, resulting in tensile stress on the machined surface.

The highest residual tensile stress on the machined surface of GH605 is obtained at the injection temperature of −90 °C, which is 347.6 MPa in the vertical feed direction and 309.3 MPa in the parallel feed direction. At this cutting condition, the machined surface is affected by both the partial thermal effect in plastic deformation and the plastic deformation after low-temperature machining. The residual tensile stress on the machined surface is greater. As the injection temperature continues to decrease, the cooling effect of liquid nitrogen keeps the cutting area in a low temperature environment. The thermal stress no longer dominates the cutting surface. And the hardness of the GH605 workpiece is improved with the reduction of injection temperature (Fig. 13), resulting in greater cutting force. The workpiece material is compressed along the vertical direction of the machined surface, and the residual tensile stress on the surface begins to decrease. It shows that the plastic deformation of the workpiece in the vertical feed direction is greater than that in the parallel feed direction. Therefore, the residual stress produced by the mechanical action in the parallel feed direction is less than that in the vertical feed direction.

The formation of tensile stress will have a certain impact on aviation structural parts. Compared with the processing of cobalt-based superalloys under dry cutting conditions, the smaller tensile residual stress is obtained by using of cryogenic LN_2 (−190 °C) in this work, which is consistent with the conclusion of cryogenic processing of Inconel 718 [38]. Due to the serious tensile residual stress on the machined surface of superalloy, there are potential risks to the fatigue strength and service life of aviation structural parts. Therefore, it is necessary to optimize the high-speed cutting process of aviation structural parts. The surface residual stress can be actively controlled by optimizing cutting parameters, tool geometric parameters and prestressed cutting [39,40]. In addition, specific surface treatment can also be performed after the cutting process to modulate the residual stress. In this work, the lower tensile stress is achieved by use of cryogenic LN_2 cutting method, which also plays a positive role in the optimization of high-speed cutting process and surface treatment of aviation structural parts.

3.6. *Liquid nitrogen injection cooling lubrication mechanism*

The influence of dry cutting on the interface between the tool and the workpiece is shown in Model Fig. 16a. In the dry cutting process, due to the lack of cutting fluid, the fresh surface is generated under the interaction between the chip bottom layer and the rake face. Without the protection of the lubricating film, it is easy to bond in the high temperature and high-pressure environment of the cutting area. As the cutting process progresses, the metal flow rate of the top layer of the chip is gradually higher than that of the bottom layer, resulting in a

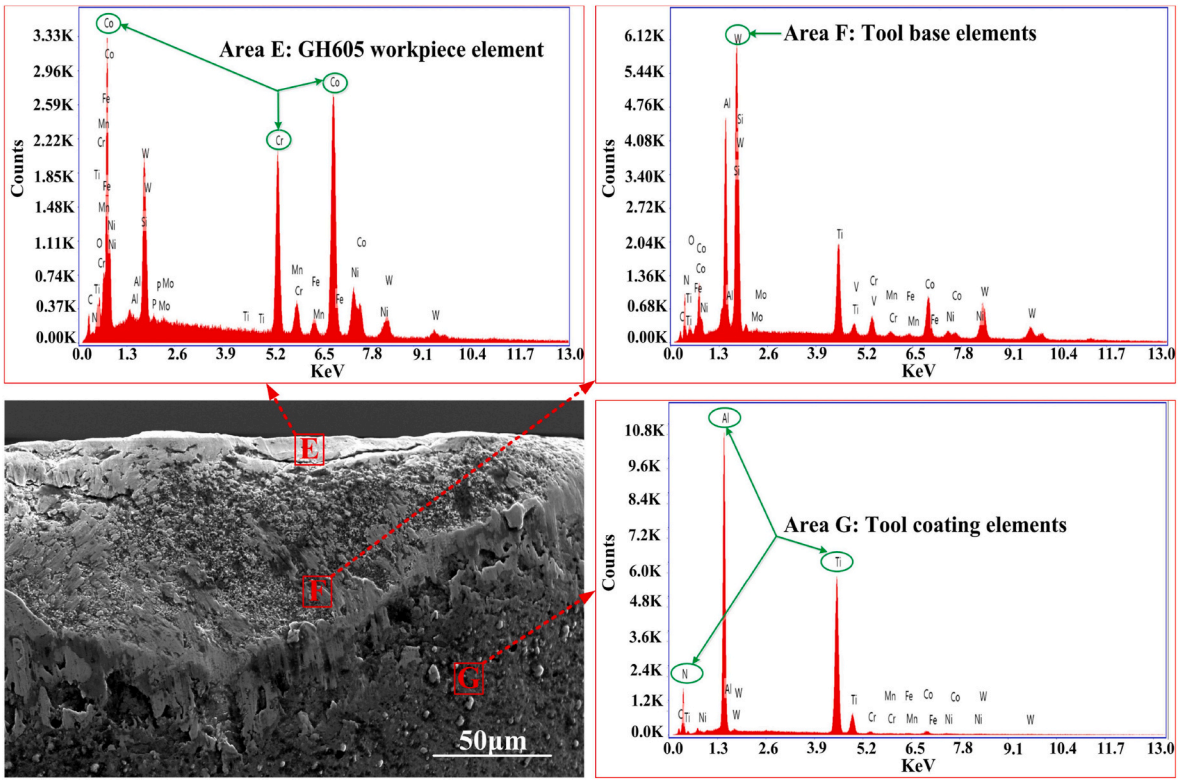

Fig. 10. Wear morphology and EDS of tool flank wear (VB = 0.180 mm) at injection temperature of −150 °C.

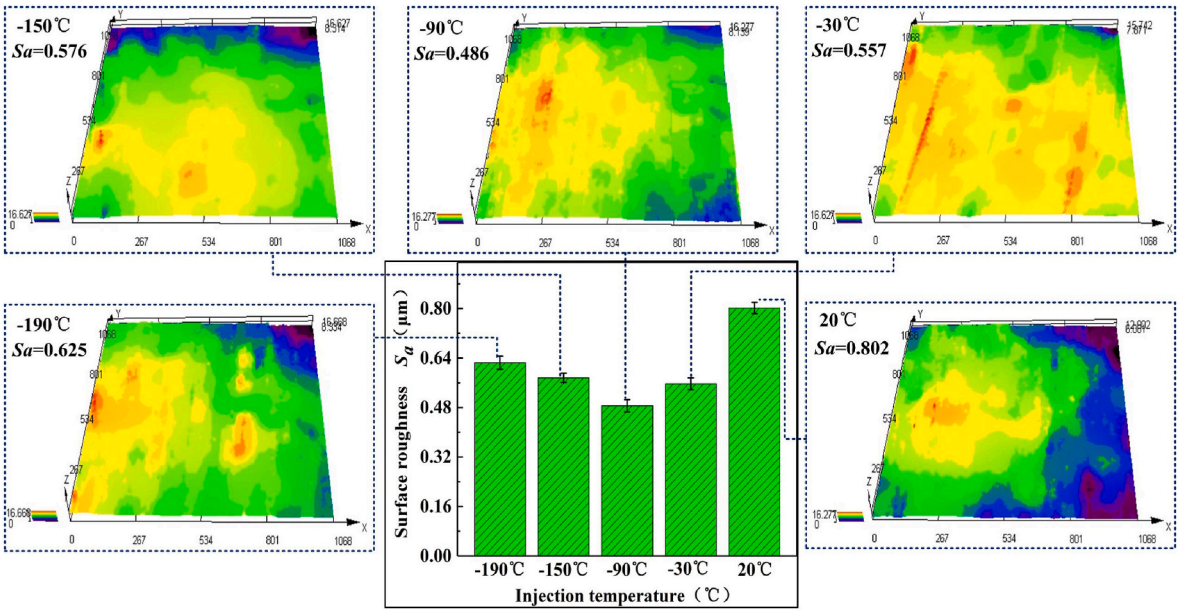

Fig. 11. Effect of injection temperature on the machined surface roughness S_a and 3D surface topography (v_c = 117 m/min, f_z = 0.09 mm, a_p = 0.2 mm, a_e = 3 mm).

shear effect.

The model of the interface lubrication effect between tool and chip is shown in Fig. 16b. In the liquid nitrogen cutting process, a stream of nitrogen or a small amount of liquid nitrogen is injected at the nozzle. The inertia of the jet forces the coolant into the capillary tube in the chip contact area. Based on capillary theory [41], the penetration of liquid nitrogen as a coolant into the tool-chip contact zone can be divided into three phases: gas-phase penetration, microdrop evaporation, and liquid-phase penetration. Firstly, the nitrogen flow enters the tool-chip contact zone as gas-phase penetration. Due to the presence of cutting heat, some of the nitrogen flow entering the capillary absorbs heat. This results in the formation of vapor-like droplets, which is microdrop evaporation. The droplets in the contact zone continue to fill the capillary, which is liquid-phase penetration. Each stage enters the capillary at a different rate and time. In cutting environments where the liquid nitrogen injection temperature is not low (≥-90 °C), the nitrogen gas flow is injected into the tool-chip contact area and a hydraulic wedge is formed between the chip and the insert. Due to the high permeability of

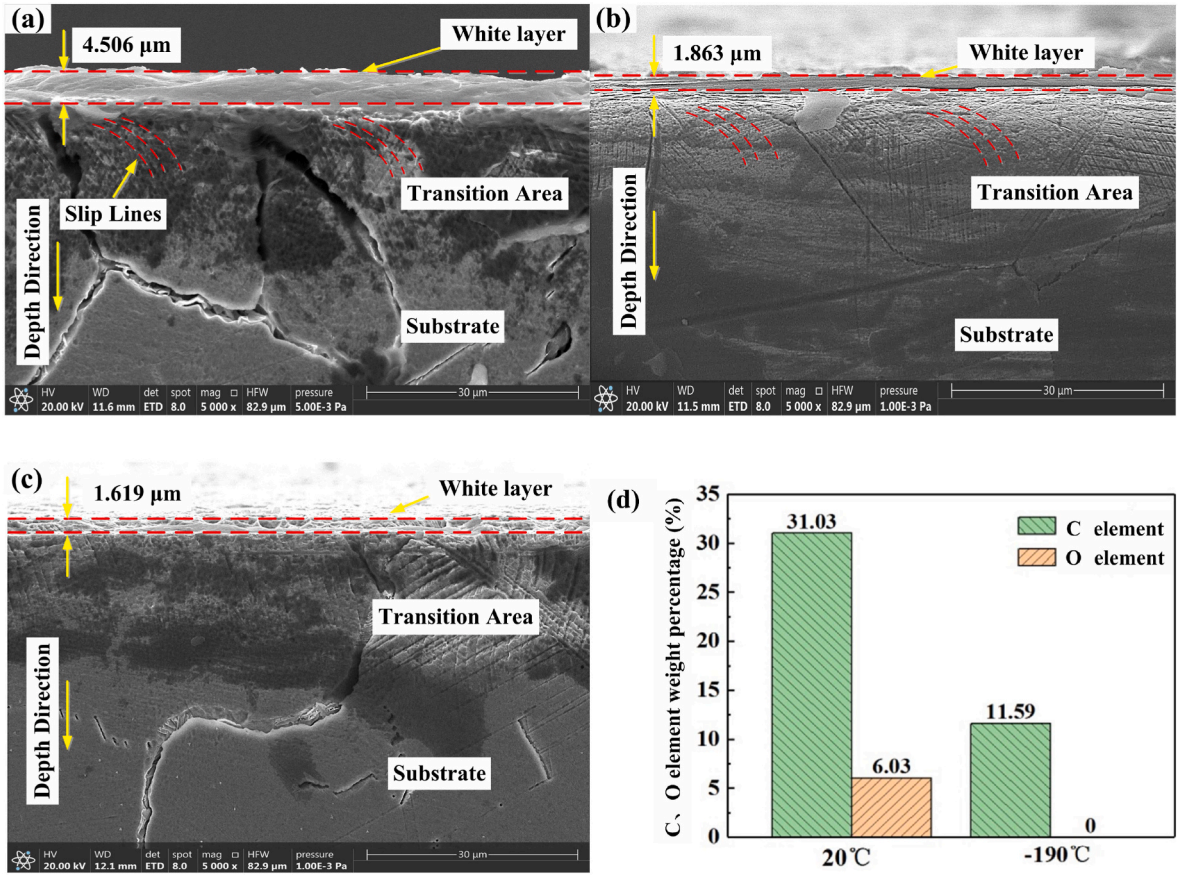

Fig. 12. Effect of injection temperature on the white layer microstructure and element weight ratio of GH605. (a) 20 °C, (b) −90 °C, (c) −190 °C and (d) Weight ratio of C and O elements in white layer.

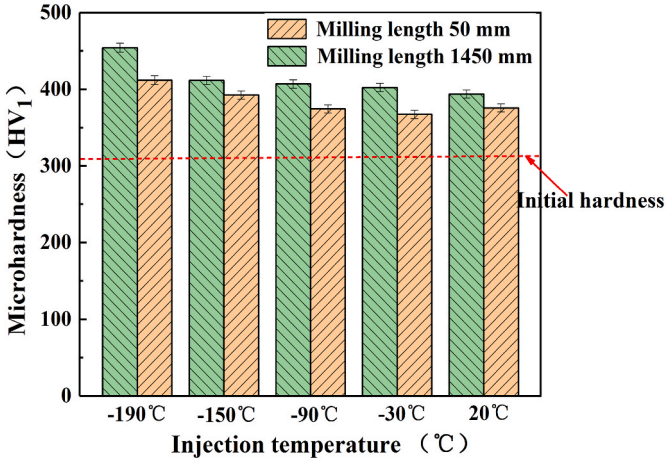

Fig. 13. Effect of injection temperature on the machined surface hardness of GH605.

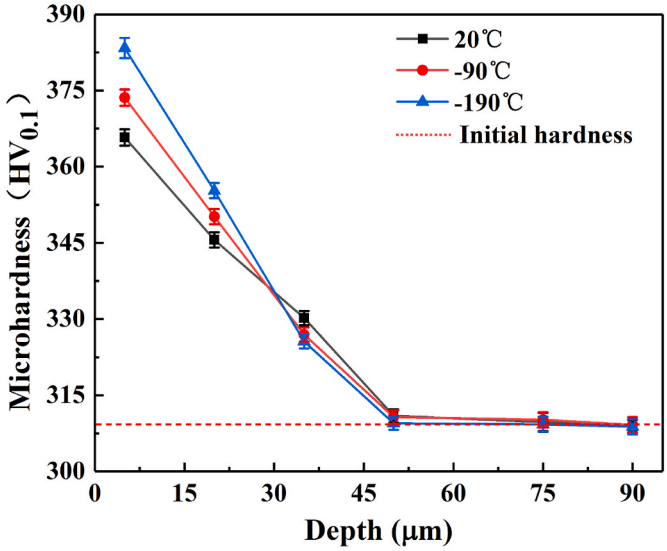

Fig. 14. Change of microhardness along the direction of work hardening depth.

the gas, a gas-liquid mixed lubrication film is quickly formed between the tool rake face and the chip and the workpiece. This reduces the direct contact between the tool and the chip and the workpiece. The cutting process due to the need for heat exchange with the surrounding environment, results in insufficient thickness or uneven distribution of the lubrication film. This makes the two mutually rubbing surfaces cannot be completely separated, thus forming the boundary lubrication phenomenon.

The interface lubrication effect model of the tool and chip is shown in Fig. 16c. As the liquid nitrogen injection temperature decreases (<-150 °C), the jet flow rate increases at very low cutting environments, and the velocity and time for each stage to enter the capillary is faster. Under the action of a huge jet flow rate cycle, the chip can be lifted by the hydraulic wedge. The hydraulic wedge in the tool-chip contact area gradually increases, the shear angle decreases, and the deformation increases. A large amount of coolant continues to penetrate the metal

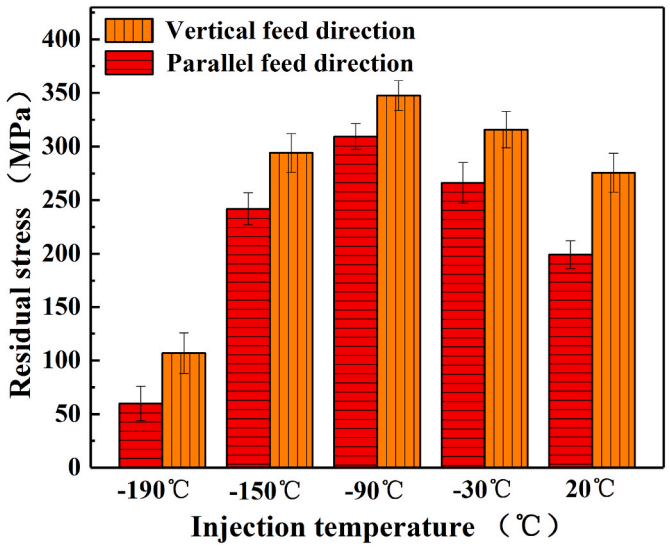

Fig. 15. Effect of injection temperature on the surface residual stress of GH605.

deformation area, effectively shortening the tool-chip contact length and taking away the heat in the cutting area in time. To achieve rapid heat absorption and cooling lubrication effect. At the same time, the free surface of chips is affected by low temperatures. And the decrease of material plasticity makes chips more prone to ductile-brittle mixed fracture.

As can be seen from Fig. 16, due to the strong permeability of the gas and the effect of gravity and pressure on the gas-liquid mixed lubrication film, it will be transmitted to the flank face through forced convection heat transfer. Thus, the flank is also affected. The heat transfer between the tool-chip contact surfaces under cryogenic cutting is achieved by a forced convective heat exchange process. This in turn improves the machinability of the material, which agrees with the study of Deshpande et al. [42] and Kale et al. [43].

4. Conclusions

(1) The influence of injection temperature on each cutting component force is basically the same. The cutting temperature decreases with the decrease of injection temperature. Due to the high cutting force and cutting temperature, dry milling leads to the shortest tool life. Under liquid nitrogen conditions, however, the lower injection temperature can greatly delay the process of the tool entering the sharp wear stage.

(2) The damage degree of the tooltip in liquid nitrogen injection cutting is reduced. With the reduction of injection temperature, the damaged area of the tool surface decreases obviously. The gas-liquid mixed protective film formed on the tool surface can effectively inhibit the generation of oxidative wear and rapid tool wear.

(3) The surface roughness S_a decreases first and then increases with the reduction of injection temperature. Compared with S_a at dry milling conditions, the surface roughness S_a is reduced by 30.55%, 39.4% and 28.18% at −30 °C, −90 °C and −150 °C, respectively. The lower surface roughness S_a can be obtained at −150 °C ~ -30 °C.

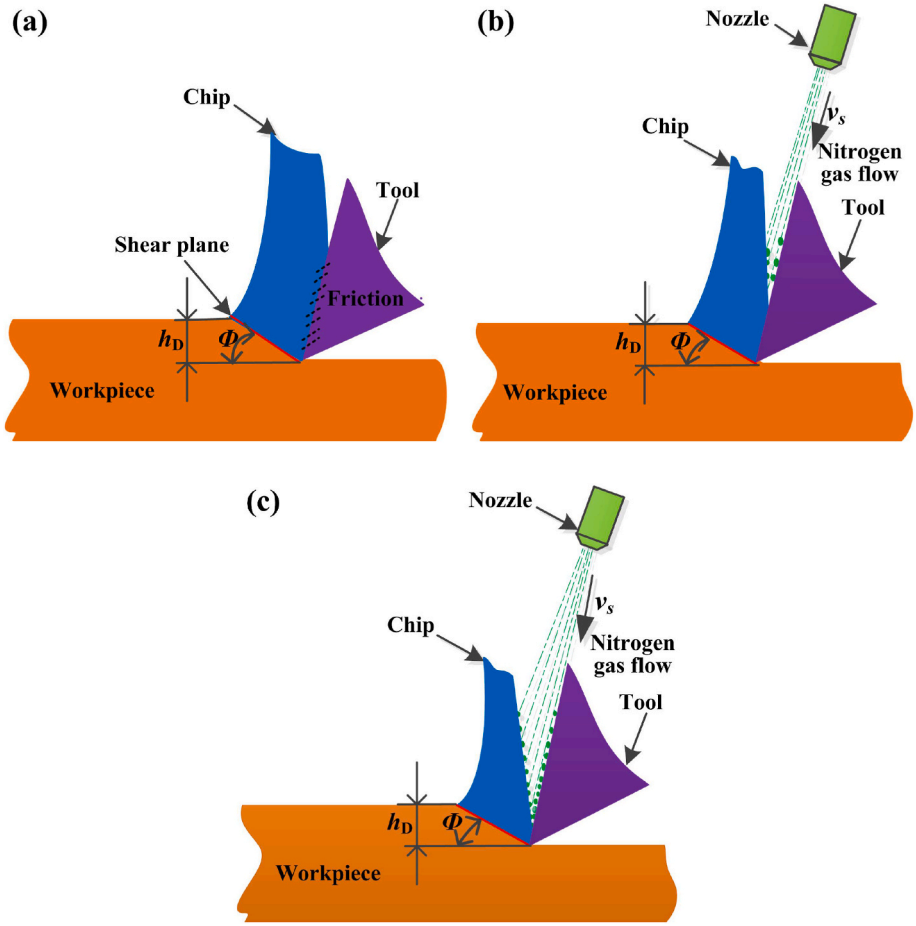

Fig. 16. Cooling lubrication model of the interface between tool and chip. (a) 20 °C, (b) −90 °C, (c) −190 °C.

(4) The white layer is presented along the depth direction, which is observed under both dry cutting and liquid nitrogen injection conditions. Under liquid nitrogen injection conditions, the thickness of the white layer is low, due to the hardly coupled by high strain and high temperature.
(5) With the decrease of injection temperature, the hardness of the machined surface shows a gradual increase. A residual tensile stress is formed on the machined surface, and the lowest residual tensile stress is obtained at −190 °C.
(6) Long tool life and a high level of machined surface integrity can be achieved at liquid nitrogen clean cutting conditions. The protective film of the gas-liquid mixture formed between the tool-chip contact surface under cryogenic cutting by injecting LN_2 enhances the effect of rapid heat absorption and cooling lubrication. It is feasible to use AlTiN coated tools for liquid nitrogen cryogenic clean cutting of cobalt-based superalloy.

During clean cutting process, the processing costs and environmental impacts are unavoidable research topics. In the following work, the machining economy and carbon emission at the same level of flank wear will be studied under the dry and LN_2 injection environment, respectively. The processing cost and environmental impact will be comprehensively evaluated and compared.

Credit author statement

Xiang Li: Conceptualization, Methodology, Formal analysis, Investigation, Writing -Original Draft, Writing - Review & Editing.
Guangming Zheng: Investigation, Formal analysis, Writing - Review & Editing, Supervision.
Jiwang Yan: Conceptualization, Writing - Review & Editing.
Xiang Cheng: Formal analysis, Writing - Review & Editing.
Yang Li: Methodology, Formal analysis.
Enzhao Cui: Investigation, Supervision.

Declaration of competing interest

The authors declare that they have no known competing financial interests or personal relationships that could have appeared to influence the work reported in this paper.

Data availability

Data will be made available on request.

Acknowledgments

This work was supported by the Natural Science Foundation of Shandong Province (No. ZR2020ME156), 2021 Innovation capability improvement project of scientific and technological small and medium-sized enterprises in Shandong Province (No. 2021TSGC1433), and Shandong Provincial Key Laboratory of Precision Manufacturing and Non-traditional Machining.

References

[1] R. Cao, H.Y. Zhang, G.H. Liu, H.Y. Che, J.H. Chen, Effect of thermal cycle shocking on microstructure and mechanical properties of Satellite 12 (Co-29Cr-2.3C-3W) cobalt based alloy, Mater. Sci. Eng., A 714 (2018) 68–74, https://doi.org/10.1016/j.msea.2017.12.057.
[2] C. Mapelli, C. Casalino, A. Strada, A. Gruttadauria, S. Barella, D. Mombelli, E. Longaretti, F. Perego, Comparison of the combined oxidation and sulphidation behavior of nickel- and cobalt-based alloys at high temperature, J. Mater. Res. Technol. 9 (2020) 15679–15692, https://doi.org/10.1016/j.jmrt.2020.11.009.
[3] M. Knezevic, J.S. Carpenter, M.L. Lovato, R.J. McCabe, Deformation behavior of the cobalt-based superalloy Haynes 25: experimental characterization and crystal plasticity modeling, Acta Mater. 63 (2014) 162–168, https://doi.org/10.1016/j.actamat.2013.10.021.
[4] L. Kuňcicka, R. Kocich', T.C. Lowe, Advances in metals and alloys for joint replacement, Prog. Mater. Sci. 88 (2017) 232–280, https://doi.org/10.1016/j.pmatsci.2017.04.002.
[5] N. Baler, P. Pandey, K. Chattopadhyay, G. Phanikumar, Influence of thermomechanical processing parameters on microstructural evolution of a gamma-prime strengthened cobalt based superalloy during high temperature deformation, Mater. Sci. Eng., A 791 (2020), 139498, https://doi.org/10.1016/j.msea.2020.139498.
[6] M. Sarıkaya, V. Yılmaz, A. Güllü, Analysis of cutting parameters and cooling/lubrication methods for sustainable machining in turning of Haynes 25 superalloy, J. Clean. Prod. 133 (2016) 172–181, https://doi.org/10.1016/j.jclepro.2016.05.122.
[7] J. Sharma, B.S. Sidhu, Investigation of effects of dry and near dry machining on AISI D2 steel using vegetable oil, J. Clean. Prod. 66 (2014) 619–623, https://doi.org/10.1016/j.jclepro.2013.11.042.
[8] S. Sartori, M. Taccin, G. Pavese, A. Ghiotti, S. Bruschi, Wear mechanisms of uncoated and coated carbide tools when machining Ti6Al4V using LN_2 and cooled N_2, Int. J. Adv. Manuf. Technol. 95 (2018) 1255–1264, https://doi.org/10.1007/s00170-017-1289-7.
[9] Y.R. Ginting, B. Boswell, W. Biswas, N. Islam, Investigation into alternative cooling methods for achieving environmentally friendly machining process, Procedia CIRP 29 (2015) 645–650, https://doi.org/10.1016/j.procir.2015.02.184.
[10] M. Kumar-Gupta, M. Mia, C.I. Pruncu, W. Kaplonek, K. Nadolny, K. Patra, Parametric optimization and process capability analysis for machining of nickel-based superalloy, Int. J. Adv. Manuf. Technol. 102 (2019) 3995–4009, https://doi.org/10.1007/s00170-019-03453-3.
[11] P. Octavio, C. Ainhoa, U. Gorka, R. Adrián, F.V. Asier, L.L. Noberto, CO_2 cryogenic milling of Inconel 718: cutting forces and tool wear, J. Mater. Res. Technol. 9 (4) (2020) 8459–8468, https://doi.org/10.1016/j.jmrt.2020.05.118.
[12] I.S. Jawahir, D.A. Puleo, J. Schoop, Cryogenic machining of biomedical implant materials for improved functional performance, life and sustainability, Procedia CIRP 46 (2016) 7–14, https://doi.org/10.1016/j.procir.2016.04.133.
[13] M.I. Sadik, S. Isakson, The role of PVD coating and coolant nature in wear development and tool performance in cryogenic and wet milling of Ti-6Al-4V, Wear 386–387 (2017) 204–210, https://doi.org/10.1016/j.wear.2017.02.049.
[14] A. Bagherzadeh, E. Kuram, E. Budak, Experimental evaluation of eco-friendly hybrid cooling methods in slot milling of titanium alloy, J. Clean. Prod. 289 (2021), 125817, https://doi.org/10.1016/j.jclepro.2021.125817.
[15] F. Pusavec, H. Hamd, J. Kopac, I.S. Jawahir, Surface integrity in cryogenic machining of nickel based alloy-Inconel 718, J. Mater. Process. Technol. 211 (2011) 773–783, https://doi.org/10.1016/j.jmatprotec.2010.12.013.
[16] N.H.A. Halim, C.H.C. Haron, J.A. Ghani, M.F. Azhar, Tool wear and chip morphology in high-speed milling of hardened Inconel718 under dry and cryogenic CO_2 conditions, Wear 426–427 (2019) 1683–1690, https://doi.org/10.1016/j.wear.2019.01.095.
[17] K. Kumark, K. Choudhurys, Investigation of tool wear and cutting forcein cryogenic machining using design of experiments, J. Mater. Process. Technol. 203 (2008) 95–101, https://doi.org/10.1016/j.jmatprotec.2007.10.036.
[18] M.J. Bermingham, J. Kirsch, S. Sun, S. Palanisamy, M.S. Dargusch, New observationson tool Life,Cutting forces and chip morphology in cryogenic MachiningTi-6Al-4V, Int. J. Mach. Tool Manufact. 51 (2011) 500–511, https://doi.org/10.1016/j.ijmachtools.2011.02.009.
[19] F.B. Wang, L.L. Li, J.K. Liu, Q.L. Shu, Research on tool wear of milling nickel-based superalloy in cryogenic, Int. J. Adv. Manuf. Technol. 91 (2017) 3877–3886, https://doi.org/10.1007/s00170-017-0079-6.
[20] F.B. Wang, Y.Q. Wang, Cleaner milling on Ti-6Al-4V alloy cooled by liquid nitrogen: external spray and inner injection, Int. J. Adv. Manuf. Technol. 112 (2021) 1193–1206, https://doi.org/10.1007/s00170-020-06440-1.
[21] M. Danish, M.K. Gupta, S. Rubaiee, A. Ahmed, M. Sarıkaya, G.M. Krolczyk, Environmental, technological and economical aspects of cryogenic assisted hard machining operation of inconel 718: a step towards green manufacturing, J. Clean. Prod. 337 (2022), 130483, https://doi.org/10.1016/j.jclepro.2022.130483.
[22] B.D. Jerold, M.P. Kumar, The influence of cryogenic coolants in machining of Ti-6Al-4V, J. Manuf. Sci. Eng. 135 (2013), 31005, https://doi.org/10.1115/1.4024058.
[23] S. Ravi, M.P. Kumar, Experimental investigations on cryogenic cooling by liquid nitrogen in the end milling of hardened steel, Cryogenics 51 (2011) 509–515, https://doi.org/10.1016/j.cryogenics.2011.06.006.
[24] S. Ravi, P. Gurusamy, Cryogenic machining of AISI p20 steel under liquid nitrogen cooling, Mater. Today: Proc. 37 (2021) 806–809, https://doi.org/10.1016/j.matpr.2020.06.005.
[25] W. Zhao, F. Ren, A. Iqbal, L. Gong, N. He, Q. Xu, Effect of liquid nitrogen cooling on surface integrity in cryogenic milling of Ti-6Al-4 V titanium alloy, Int. J. Adv. Manuf. Technol. 106 (2020) 1497–1508, https://doi.org/10.1007/s00170-019-04721-y.
[26] Q.H. Jiang, Z.C. Liu, T. Li, W.L. Cong, H.C. Zhang, Emergy-based life-cycle assessment (Em-LCA) for sustainability assessment: a case study of laser additive manufacturing versus CNC machining, Int. J. Adv. Manuf. Technol. 102 (2019) 4109–4120, https://doi.org/10.1007/s00170-019-03486-8.
[27] N. Khanna, A. Rodríguez, P. Shah, O. Pereira, A.R. Mateos, L.N.L. Lacalle, T. Ostra, Comparison of dry and liquid carbon dioxide cutting conditions based on machining performance and life cycle assessment for end milling GFRP, Int. J. Adv. Manuf. Technol. 122 (2022) 821–833, https://doi.org/10.1007/s00170-022-09843-4.
[28] A.H. Tazehkandi, M. Shabgard, G. Kiani, F. Pilehvariane, Investigation of the influences of polycrystalline cubic boron nitride (PCBN) tool on the reduction of

cutting fluid consumption and increase of machining parameters range in turning Inconel 783 using spray mode of cutting fluid with compressed air, J. Clean. Prod. 135 (2016) 1637–1649, https://doi.org/10.1016/j.jclepro.2015.12.102.
[29] J. Thrinadh, D. Saurav, M. Manoj, Influence of cutting tool material on machinability of Inconel 718 superalloy, Mach. Sci. Technol. 25 (2021) 349–397, https://doi.org/10.1080/10910344.2020.1815047.
[30] N.H.A. Halim, C.H.C. Haron, J.A. Ghani, PVD multi-coated carbide milling inserts performance: comparison between cryogenic and dry cutting conditions, J. Manuf. Process. 73 (2022) 895–902, https://doi.org/10.1016/j.jmapro.2021.11.033.
[31] S. Ş irin, Ç.V. Yıldırım, T. Kıvak, Performance of cryogenically treated carbide inserts under sustainable cryo-lubrication assisted milling of Inconel X750 alloy, Sustain. Mater. Technologies. 29 (2021), e00314, https://doi.org/10.1016/j.susmat.2021.e00314.
[32] D. Fernández, A. Sandá, I. Bengoetxea, Cryogenic milling: study of the effect of CO_2 cooling on T ool wear when machining inconel 718, grade EA1N steel and gamma TiAl, Lubricants 7 (2019) 10, https://doi.org/10.3390/lubricants7010010.
[33] Y. Li, G.M. Zheng, X. Cheng, X.H. Yang, R.F. Xu, H.Q. Zhang, Cutting performance evaluation of the coated tools in high-speed milling of AISI 4340 steel, Materials 12 (2019) 3266, https://doi.org/10.3390/ma12193266.
[34] S. Pervaiz, S. Kannan, S. Anwar, Machinability analysis of dry and liquid nitrogen–based cryogenic cutting of Inconel 718: experimental and FE analysis, Int. J. Adv. Manuf. Technol. 118 (2022) 3801–3818, https://doi.org/10.1007/s00170-021-08173-1.
[35] A.H. Musfirah, J.A. Ghani, C.H.C. Haron, Tool wear and surface integrity of Inconel 718 in dry and cryogenic coolant at high cutting speed, Wear 376–377 (2017) 125–133, https://doi.org/10.1016/j.wear.2017.01.031.
[36] A. la Monaca, J.W. Murray, Z.R. Liao, A. Speidel, J.A. Robles-Linares, D.A. Axinte, M.C. Hardy, A.T. Clare, Surface integrity in metal machining - Part II: functional performance, Int. J. Mach. Tool Manufact. 164 (2021), 103718, https://doi.org/10.1016/j.ijmachtools.2021.103718.
[37] S. Chaabani, P.J. Arrazola, Y. Ayed, A. Madariaga, A. Tidu, G. Germain, Comparison between cryogenic coolants effect on tool wear and surface integrity in finishing turning of Inconel 718, J. Mater. Process. Technol. 285 (2020), 116780, https://doi.org/10.1016/j.jmatprotec.2020.116780.
[38] Z.H. He, X.M. Zhang, H. Ding, Comparison of residual stresses in cryogenic and dry machining of inconel 718, Procedia CIRP 46 (2016) 19–22, https://doi.org/10.1016/j.procir.2016.03.130.
[39] R.T. Peng, K.F. Liu, X.Z. Tang, M. Liao, Y.L. Hu, Effect of prestress on cutting of nickel-based superalloy GH4169, Int. J. Adv. Manuf. Technol. 100 (2019) 813–825, https://doi.org/10.1007/s00170-018-2746-7.
[40] R.T. Peng, F. Lu, X.Z. Tang, Y.Q. Tan, 3D finite element analysis of prestressed cutting, Adv. Mater. Res. 591–593 (2012) 766–770. https://doi.org/10.4028/www.scientific.net/AMR.591-593.766.
[41] V.A. Godleviski, A.V. Volkov, The kinetics of lubricant penetration action during machining, Lubric. Sci. 9 (1997) 127–140, https://doi.org/10.1002/ls.3010090203.
[42] Y.V. Deshpande, A.B. Andhare, P.M. Padole, How cryogenic techniques help in machining of nickel alloys? A review[J], Mach. Sci. Technol. 22 (4) (2018) 543–584, https://doi.org/10.1080/10910344.2017.1382512.
[43] A. Kale, N. Khanna, A review on cryogenic machining of super alloys used in aerospace industry, J]. Procedia. Manuf. 7 (2017) 191–197, https://doi.org/10.1016/j.promfg.2016.12.047.